

Antimetastatic Activity of Honokiol in Osteosarcoma

Patrick Steinmann, MD, MSc¹; Denise K. Walters, PhD¹; Matthias J. E. Arlt, PhD¹; Ingo J. Banke, MD¹; Urs Ziegler, PhD²; Bettina Langsam, TA¹; Jack Arbiser, MD, PhD^{3,4}; Roman Muff, PhD¹; Walter Born, PhD¹; and Bruno Fuchs, MD, PhD¹

BACKGROUND: Metastasizing osteosarcoma has a mean 5-year survival rate of only 20% to 30%. Therefore, novel chemotherapeutics for more effective treatment of this disease are required. **METHODS:** The antineoplastic activity of honokiol, which was demonstrated previously in numerous malignancies, was studied in vivo in C3H mice subcutaneously injected with syngeneic β -galactosidase bacterial gene (*lacZ*)-expressing LM8 osteosarcoma (LM8-*lacZ*) cells. In vitro cytotoxic effects of honokiol were investigated in 8 human and 2 murine osteosarcoma cell lines with different in vivo metastatic potential. **RESULTS:** Seven days after subcutaneous flank injection of LM8-*lacZ* cells, daily intraperitoneal treatment of mice with 150 mg/kg honokiol reduced the number of micrometastases in the lung by 41% and reduced the number of macrometastases in the lung and liver by 69% and 80%, respectively, compared with control. Primary tumor growth was not inhibited. In osteosarcoma cell lines, honokiol inhibited the metabolic activity with a half-maximal concentration (IC₅₀) between 8.0 μ g/mL and 16 μ g/mL. Cyclosporin A partially reversed the inhibition of metabolic activity in LM8-*lacZ* cells. Cell proliferation and wound healing migration of LM8-*lacZ* cells were inhibited by honokiol with an IC₅₀ between 5.0 μ g/mL and 10 μ g/mL. Higher concentrations caused rapid cell death, which was distinct from necrosis, apoptosis, or autophagy but was associated with swelling of the endoplasmic reticulum, cytoplasmic vacuolation, and morphologically altered mitochondria. **CONCLUSIONS:** Honokiol exhibited prominent antimetastatic activity in experimental osteosarcoma and caused rapid cell death in vitro that was unrelated to necrosis, apoptosis, or autophagy. The authors concluded that honokiol has considerable potential for the treatment of metastasizing osteosarcoma. *Cancer* 2012;118:2117-27. © 2011 American Cancer Society.

KEYWORDS: cytotoxicity, honokiol, metastasis, osteosarcoma.

INTRODUCTION

Osteosarcoma is the most common primary malignant bone tumor predominantly occurring in childhood and adolescence. Current therapy includes surgical tumor resection and multiagent chemotherapy. The introduction of (neo)-adjuvant chemotherapy has increased the 5-year survival rate for localized disease by greater than 50% compared with surgery alone. In contrast, patients who present with metastases at diagnosis continue to have a poor prognosis with 5-year survival rates of 20% to 30%.^{1,2} Moreover, currently approved agents exhibit major side effects (for reviews, see Longhi et al and Marina et al^{1,2}). Thus, the development of novel agents with increased efficiency and reduced toxicity for the treatment of osteosarcoma and metastatic disease in particular is essential.

Honokiol, a biphenolic compound present in Magnolia tree extracts, has been used for centuries in traditional Chinese and Japanese medicine to treat anxiety, thrombotic stroke, and gastrointestinal symptoms. Cardioprotective,^{3,4} antimicrobial,⁵ anti-inflammatory,^{6,7} and antiangiogenic^{8,9} properties also have been reported. It is noteworthy that honokiol has demonstrated antineoplastic properties in vitro against a variety of cancers.⁸⁻¹⁸ Furthermore, honokiol was effective in vivo in angiosarcoma,⁸ colorectal carcinoma,¹⁴ breast cancer,¹⁷ and gastric cancer¹⁸ and inhibited bone metastasis in a murine prostate cancer model.¹⁶ Moreover, honokiol potentiated the effects of various other chemotherapeutic drugs in vitro^{9,11,16} and in vivo¹⁶ and demonstrated the ability to overcome chemoresistance in human multiple myeloma cells.⁹ Several studies with tumor cells suggested that the cytotoxicity of honokiol is brought about predominantly through

Corresponding author: Bruno Fuchs, MD, PhD, Department of Orthopedics, Balgrist University Hospital, Forchstrasse 340, 8008 Zurich, Switzerland; Fax: (011) 41-44-386-1669; research@balgrist.ch

¹Laboratory for Orthopedic Research, Department of Orthopedics, University of Zurich, Switzerland; ²Center for Microscopy and Image Analysis, University of Zurich, Switzerland; ³Emory University School of Medicine, Atlanta, Georgia; ⁴Atlanta Veterans Administration Medical Center, Atlanta, Georgia

The first 3 authors contributed equally to this article.

DOI: 10.1002/cncr.26434, **Received:** March 17, 2011; **Revised:** June 15, 2011; **Accepted:** June 16, 2011, **Published online** September 20, 2011 in Wiley Online Library (wileyonlinelibrary.com)

activation of distinct apoptotic mechanisms.^{8,9,13,14,16} Honokiol is well tolerated,^{8,14,16} has good bioavailability in vivo,¹⁴ and is available orally,^{19,20} making it an attractive novel agent for the treatment of patients with osteosarcoma.

In the current study, the antineoplastic properties of honokiol were examined in the syngeneic LM8/C3H mouse osteosarcoma model.^{21,22} Mice that were injected subcutaneously into the flank with β -galactosidase bacterial gene (*LacZ*)-transduced LM8 (LM8-*LacZ*) cells, developed local primary tumors, which metastasized to lung and liver. Daily intraperitoneal treatment of the mice with honokiol inhibited metastasis to both lung and liver. The promising antineoplastic activity of honokiol observed in this mouse osteosarcoma model was investigated further in vitro in 1 more mouse cell line and in 8 human osteosarcoma cell lines with differing metastatic activities. Mechanistically, the cytotoxic effects of honokiol in LM8 cells were investigated by transmission electron microscopy.

MATERIALS AND METHODS

Tissue Culture and Reagents

The human osteosarcoma cell lines SAOS-2 (HTB-85), HOS, and 143B and the human embryonic kidney cell line HEK293-T were obtained from the American Type Culture Collection (Rockville, Md). SAOS-2-derived LM5 cells were provided by E. S. Kleinerman (The University of Texas M. D. Anderson Cancer Center, Houston, Tex). The human osteosarcoma MG-63 cell line was obtained from G. Sarkar (Mayo Clinic, Rochester, Minn), and the MG-63 M8 cell subline was obtained from W. T. Zhu (Tongji Hospital, Huazhong University of Science and Technology, Wuhan, China). The mouse osteosarcoma cell lines Dunn and LM8 were provided by T. Ueda (Osaka National Hospital, Osaka, Japan). All of these cell lines were cultured in Dulbecco Modified Eagle Medium/Ham F12 medium (1:1 dilution; Invitrogen, Carlsbad, Calif) containing 10% fetal calf serum (tissue culture medium), 1 U/mL penicillin G, and 1 μ g/mL streptomycin (Invitrogen). The human osteosarcoma cell lines HU09 and HU09 M132 were provided by M. Tani (National Cancer Center Hospital, Tokyo, Japan) were grown in RPMI medium (Invitrogen) supplemented with 10% fetal calf serum, 1 U/mL penicillin G, and 1 μ g/mL streptomycin. All cells were cultured in a tissue culture incubator at 37°C in a humidified atmosphere of 5% CO₂.

Honokiol and cyclosporin A were purchased from Sigma-Aldrich Chemical Company (St. Louis, Mo).

Antineoplastic Activity of Honokiol in the LM8 Mouse Osteosarcoma Model

Eight-week-old female C3H/HeNCrl mice (20 g average body weight) obtained from Charles River Laboratories (Wilmington, Mass) were housed according to the guidelines of the Federal Veterinary Office (FVO) and the experiments were approved by the authorities of the Canton of Zurich. Syngeneic LM8 osteosarcoma cells were transduced retrovirally with a cytomegalovirus promoter-driven *lacZ* gene (LM8-*lacZ* cells) to facilitate and improve their identification and localization in primary tumors and metastases as reported previously.²³ On experimental day 0, 10⁷ LM8-*lacZ* cells in 200 μ L phosphate-buffered saline were injected subcutaneously into the left flank of the mice. On experimental day 7, the length and width of the primary tumors were measured with a caliper, and the tumor volume (length \times width²/2) was calculated. The mice were then divided randomly into 2 groups of equal number, which were treated daily with intraperitoneal honokiol (150 mg/kg) in 300 μ L Intralipid (vehicle) (Fresenius Kabi, Bad Homburg, Germany) or with 300 μ L vehicle alone. The health of the mice was monitored daily, and the tumor size was measured once weekly. On experimental day 25, the mice were killed, and the primary tumor, the lungs, and the liver were prepared as recently reported.²³ The left lobe of the lung and the 2 upper and the middle lobes of the liver were stained with 5-bromo-4-chloro-3-indolyl- β -D-galactoside (X-gal), and the *lacZ*-expressing metastases were quantified as described below.

Quantification of LM8-LacZ Cell-Derived Lung and Liver Metastases

Tissues were treated as described previously.²³ Stained lungs and livers were photographed with a Kappa PS 20 C digital camera (Kappa Opto-Electronics GmbH, Gleichen, Germany) connected to an OpMi-1 binocular microscope (Carl Zeiss, Oberkochen, Germany), and the images were imported as TIF files into Power Point software (Microsoft Inc., Redmond, Wash). Then, macro-metastases on organ surfaces, defined as indigo blue-stained foci >0.1 mm in greatest dimension, were counted. Micrometastases on organ surfaces, defined as indigo blue-stained foci <0.1 mm in greatest dimension, were counted in 10 randomly selected close-up images of individual organs in an area of 1 mm² defined by a

superimposed counting grid. Close-up images of 10 mm² were taken with the Kappa PS 20 C digital camera connected to an Eclipse E600 microscope (Nikon Corporation, Tokyo, Japan) and imported as TIF files into Power Point software.

Metabolic Proliferation Assay

Individual cell lines that had been seeded into 96-well plates at a density of 3000 cells per well and grown overnight were incubated for indicated periods in the absence or presence of honokiol at indicated concentrations. A potential protective action of cyclosporine A counteracting the cytotoxic activity of honokiol was investigated in cells that were seeded at 5000 to 10,000 cells per well and grown for 24 hours. The cells were preincubated for 2 hours with 10 μM cyclosporin A and then incubated for 2 hours with honokiol in the presence of cyclosporin A. The metabolic activity of drug-treated and nontreated cells was assessed after 2 to 3 hours of incubation with 10 μL per well WST-1 reagent (Roche Diagnostics Corp., Indianapolis, Ind), which is cleaved to formazan by mitochondrial dehydrogenases in metabolizing cells. Formazan was quantified at 415 nm with a scanning multiwell spectrophotometer (Bio-Rad, Hercules, Calif). Metabolic activity was expressed as the percentage of formazan formation in honokiol-treated cells compared with the percentage of formation in untreated control cells set to 100%. The half-maximal growth inhibitory concentration (IC₅₀) of honokiol was calculated with Prism 4 network software (GraphPad Software, Inc., San Diego, Calif).

Proliferation Assay

For the proliferation assay, 10⁵ LM8-*lacZ* cells were seeded in 12.5-cm² flasks. After adhesion for 3 hours, the cells were treated or were left untreated (control cells) at the indicated concentrations of honokiol for 45 hours. Nontreated control cells reached approximately 50% confluence. The total number of cells per flask was counted with a Neubauer chamber. The recovery of the cells from honokiol treatment was assessed by seeding the remaining cells at a density of <10⁵ cells per 25-cm² flask. Cells treated with ≤10 μg/mL honokiol or with 12.5 μg/mL to 20 μg/mL honokiol were then allowed to grow in the absence of honokiol for 3 days or for up to 11 days, respectively, and then were counted as described above. Doubling times (t_{1/2}; hours) were calculated according to the equations $N = N_0 e^{kt}$ and $t_{1/2} = \ln 2/k$ (N = cell number; N_0 = number of seeded cells; t = time; k = variable parameter).

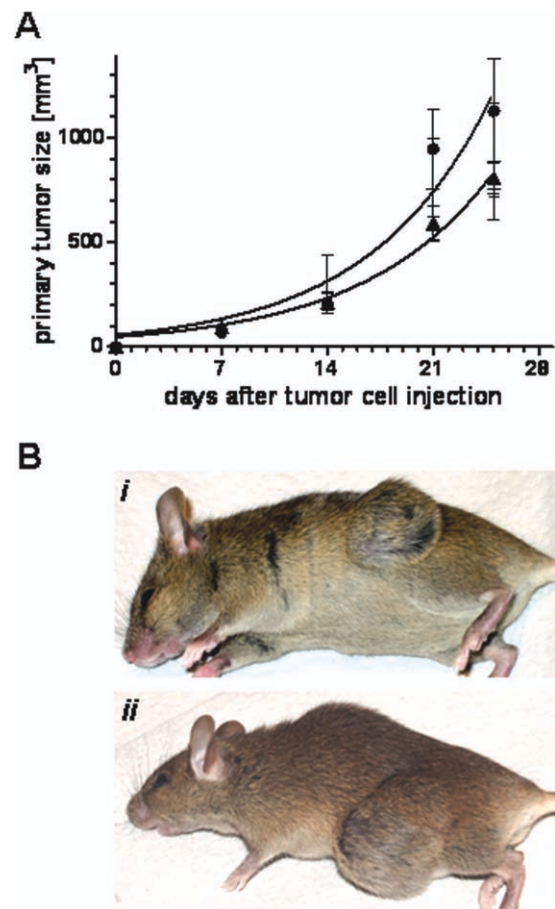


Figure 1. Honokiol does not affect subcutaneous primary tumor growth of β -galactosidase bacterial gene (*lacZ*)-expressing LM8 mouse osteosarcoma (LM8-*lacZ*) cells in syngeneic C3H mice. (A) Mice were treated daily with intraperitoneal injections of vehicle (triangles) or 150 mg/kg honokiol (circles). Data are expressed as the mean \pm standard error of the mean ($n = 9$; $P > .05$ at all time points). (B) These are representative images of LM8-*lacZ* cell-derived subcutaneous tumors in C3H mice that were treated daily with (i) vehicle or (ii) 150 mg/kg honokiol.

Wound-Healing Migration Assay

Cells were seeded into 24-well plates at approximately 40% confluence. At confluence, the cells were preincubated in the absence (control) or in the presence of indicated concentrations of honokiol at 37°C for 3 hours. A wound that measured between 0.6 mm and 1 mm in width and approximately 1 cm in length was then applied, and cell debris was removed by washing with tissue culture medium. Homogenous wound areas were marked with a Nikon object marker attached to a Nikon Diaphot microscope (Fig. 1B). The widths of the wounds in marked areas were measured with a Nikon ocular with a graded 1-mm scale immediately after wounding (D_0) and after

further incubation under prewounding conditions for 20 hours (D_t). Migration rates ($\mu\text{m}/\text{hour}$) were calculated with the equation $(D_o - D_t)/2 \times 20$ hours.

Microscopic Examination of Honokiol-Evoked Vacuolation

Cells were seeded (1:10) on coverslips in 24-well plates and allowed to grow for 2 days. After preincubation in the absence or in the presence of 10 μM cyclosporin A, the cells were incubated with 15 $\mu\text{g}/\text{mL}$ honokiol for 2 hours and then fixed with 10% formalin for 10 minutes. Then, the cells were mounted with ImmuMount (Thermo Scientific, Fremont, Calif) and photographed with an Axio-Cam MrC camera (Zeiss) attached to a Zeiss Observer.Z1 microscope with a $\times 40$ objective.

Transmission Electron Microscopy

Cells were seeded on carbon-coated cover slides in 6-well plates at a density of 10,000 cells per cm^2 and allowed to adhere for 24 hours. Then, the cells were left untreated or were treated with 15 $\mu\text{g}/\text{mL}$ honokiol for either 1.5 hours or 6 hours. Cells were first fixed with 2.5% glutaraldehyde and sequentially treated with 1% OsO_4 and 1.5% $\text{K}_4\text{Fe}(\text{CN})_6$ in 100 mM sodium phosphate, pH 7.2, for 30 minutes. The cells were dehydrated in an ethanol series and embedded in Epon (Catalys, Dubendorf, Switzerland). Ultrathin (50 nm) sections were contrasted with uranyl acetate and lead citrate and were examined with a CM100 transmission electron microscope (Philips, Amsterdam, the Netherlands).

Statistical Analysis

The results are presented here as means \pm standard errors of the mean. Statistical analysis of in vivo data was performed with the Mann-Whitney rank-sum test, and the t test was used to analyze in vitro data. P values $< .05$ were considered statistically significant.

RESULTS

Honokiol Inhibits Spontaneous Lung and Liver Metastasis but Does Not Inhibit Primary Tumor Growth

In the current study, the antineoplastic properties of honokiol were examined in a syngenic LM8 mouse osteosarcoma model. In this model, subcutaneous inoculation of LM8-*lacZ* cells in the flank of C3H mice resulted in the formation of local primary tumors and spontaneous metastasis, predominantly to the lung and the liver. Indeed, all mice injected with 1×10^7 LM8-*lacZ* cells developed

local primary tumors within 7 days and had an average tumor volume of $79.9 \pm 5.7 \text{ mm}^3$. Subsequent daily intraperitoneal bolus injections of 150 mg/kg honokiol did not inhibit progressive primary tumor growth. The increase in tumor volume over time was indistinguishable in honokiol-treated mice and vehicle-treated mice (Fig. 1). At sacrifice, tumors in honokiol-treated mice appeared even slightly larger than those in untreated animals and tumor necrosis was not observed (results not shown).

However, the antimetastatic activity of honokiol became evident when spontaneous metastasis of LM8-*lacZ* cells to the lung and the liver were compared in tumor-bearing, honokiol-treated mice and in vehicle-treated control animals. The mean number of X-gal-stained macrometastases (>0.1 mm in greatest dimension) on lung surfaces decreased significantly by $69.6\% \pm 9.2\%$ from 116.5 ± 14.9 macrometastases in vehicle-treated control mice to 35.4 ± 10.7 macrometastases in honokiol-treated animals ($P < .01$) (Fig. 2). The mean number of micrometastases (<0.1 mm in greatest dimension) per 10 mm^2 lung surface also decreased significantly ($P < .05$) by $41.4\% \pm 7.3\%$ from 202 ± 21 micrometastases in control mice to 118 ± 27 micrometastases in honokiol-treated animals. In the liver, honokiol treatment reduced the mean number of macrometastases even more effectively than in the lung by $>80\%$ from 40.5 ± 9.8 lesions in control mice to 8.0 ± 2.4 lesions in honokiol-treated animals ($P < .01$), but the number of micrometastases was not significantly reduced. Remarkably, the density of micrometastases on the liver surface of untreated mice was $<10\%$ of the density on the surface of the lungs.

Honokiol Inhibits the Metabolic Activity of Osteosarcoma Cell Lines in Vitro

In 1977, Fidler and Kripke²⁴ proposed that primary tumors of various malignancies, including osteosarcoma, are comprised of heterogeneous cell populations, which, we now know, vary in both gene expression pattern and degree of malignancy. Consequently, next, we wanted to examine the in vitro effect of honokiol on 8 human and 2 murine osteosarcoma cell lines that possess low and high metastatic activity and distinct gene expression profiles (unpublished observations).

The cytotoxic effects of honokiol were examined with the WST-1 assay, which indicates the metabolic activity of viable cells. The different cell types were treated with honokiol for 72 hours according to protocols from studies that established the antineoplastic activity of this natural compound in other tumor types. Honokiol

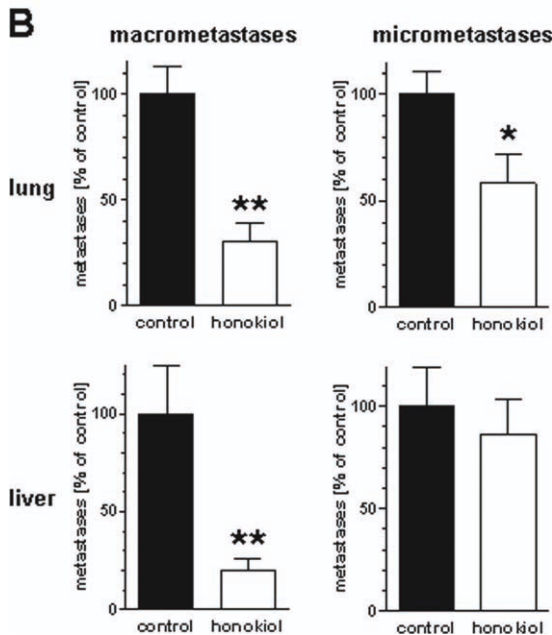
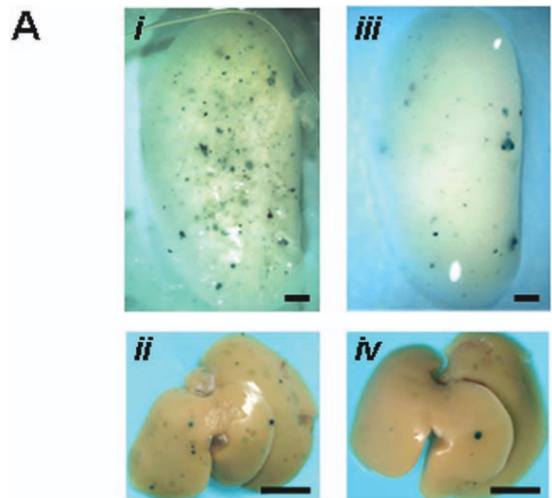


Figure 2. Honokiol inhibits metastasis of β -galactosidase bacterial gene (*lacZ*)-expressing LM8 mouse osteosarcoma (LM8-*lacZ*) cells to the lung and the liver. (A) These are representative photographs of 5-bromo-4-chloro-3-indolyl- β -D-galactoside (X-gal)-stained metastases in whole mounts of (i, iii) lungs and (ii, iv) livers in (i, ii) vehicle-treated mice and (iii, iv) honokiol-treated mice. Scale bars = 1 mm in i and iii, 5 mm in ii and iv. (B) The percentage of macrometastases (>0.1 mm) and micrometastases (<0.1 mm) on lung and liver surfaces in honokiol-treated mice (n = 9) are compared with the mean number of respective metastases set to 100% in vehicle-treated control animals (n = 9). Data are expressed as the mean \pm standard error of the mean compared with controls. A single asterisk indicates $P < .05$; double asterisks, $P < .01$.

Table 1. Half-Maximal Growth Inhibitory Concentrations of Honokiol in Human and Mouse Osteosarcoma Cell Lines

Cell Line ^a	IC ₅₀ , $\mu\text{g/mL}$
HUO9	15.8
HUO9 M132 ^b	8.5
HOS	13.7
143B ^c	11.1
MG-63	9.3
MG-63 M8 ^d	9.3
SAOS-2	12.9
LM5 ^e	8.0
Dunn	9.6
LM8 ^f	8.3

Abbreviations: IC₅₀, half-maximal growth inhibitory concentration.

^aAll cell lines were treated with honokiol for 72 hours. The results are means from at least 4 independent experiments performed in triplicate.

^bHUO9 is a highly metastatic subline of the parental HUO9 cell line.

^c143B is a highly metastatic subline of the parental HOS cell line.

^dMG-63 M8 is a highly metastatic subline of the parental MG-63 cell line.

^eLM5 is a highly metastatic subline of the parental SAOS-2 cell line.

^fLM8 is a highly metastatic subline of the parental Dunn cell line.

inhibited the metabolic activity of all osteosarcoma cell lines at comparable IC₅₀ values between 8.0 $\mu\text{g/mL}$ and 16 $\mu\text{g/mL}$ (Table 1).

Honokiol Inhibits Proliferation and Migration of LM8-*lacZ* Cells

Our observation that the cytotoxic effects of honokiol were relatively similar among our diverse panel of osteosarcoma cell lines suggested that honokiol must affect a common target(s) within these cells. Consequently, the LM8-*lacZ* cell line, which also was used in our murine osteosarcoma model, was considered representative of all of the other cell lines and, thus, was used in all subsequent experiments designed to further elucidate the antineoplastic action of honokiol.

Treatment of LM8-*lacZ* cells with honokiol for 45 hours inhibited proliferation dose-dependently with an IC₅₀ of approximately 5 $\mu\text{g/mL}$ (Fig. 3A). The calculated doubling time of 14.0 ± 0.2 hours (n = 8) in nontreated LM8-*lacZ* cells increased to 23.9 ± 1.1 hours (n = 7; $P < .0001$) in cells that were treated with 5 $\mu\text{g/mL}$ honokiol, and an almost complete inhibition of proliferation was observed at a concentration of 10 $\mu\text{g/mL}$ honokiol. Concentrations >10 $\mu\text{g/mL}$ lowered the number of surviving cells below the number of seeded cells because of cell death.

The recovery of LM8-*lacZ* cells from the 45-hour honokiol treatment was assessed after reseeding and culturing the cells between 3 days and 11 days in the absence of honokiol. Cells that were treated with up to 10 $\mu\text{g/mL}$ honokiol demonstrated post-treatment doubling times that were indistinguishable from those of naive LM8-*lacZ*

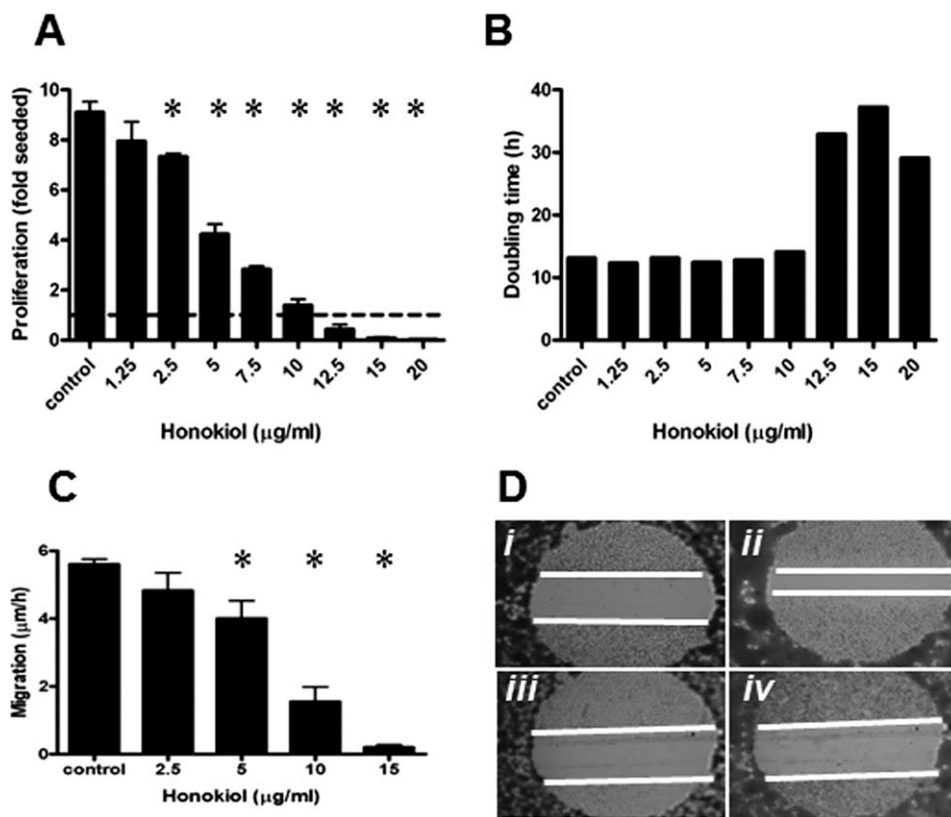


Figure 3. Honokiol inhibits proliferation and wound healing migration of β -galactosidase bacterial gene (*lacZ*)-expressing LM8 mouse osteosarcoma (LM8-*lacZ*) cells. (A) This chart illustrates the dose-dependent inhibition of LM8-*lacZ* cell proliferation by honokiol. In this experiment, 8000 cells/cm² were seeded, allowed to adhere for 3 hours, and then incubated in the absence (control) or presence of the indicated concentrations of honokiol for 45 hours. Proliferation is indicated as the fold increase in cell number normalized to the number of seeded cells indicated by the dashed line. Results are expressed as the means \pm standard error of the mean of 3 independent experiments that were carried out in duplicate. Asterisks indicate $P < .05$ compared with control. (B) This bar chart illustrates the recovery of proliferation after treatment with honokiol for 48 hours. Honokiol-treated cells were allowed to recover, and the doubling times were calculated as described in the text (see Materials and Methods). The results are expressed as the means \pm standard error of the mean of 2 independent experiments. (C) This chart illustrates dose-dependent inhibition of the migration rate by honokiol. Cells were treated for 23 hours with the indicated concentrations of honokiol, and the migration rates were determined as outlined in the text (see Materials and Methods). Results are expressed as the means \pm standard error of the mean from 4 independent experiments that were carried out in triplicate. Asterisk indicate $P < .05$ compared with controls. (D) These are views of representative wounds that were examined microscopically (i, iii) immediately after wounding and after incubation for 20 hours (ii) in the absence or (iv) in the presence of 15 μ g/mL honokiol.

cells (Fig. 3B), suggesting that these cells had fully recovered from treatment with honokiol. Cells that were treated with honokiol concentrations >10 μ g/mL, conversely, recovered poorly with doubling times that were 2-fold to 3-fold higher compared with the doubling times in untreated cells.

The effect of honokiol on migration, which is considered an indicator of metastatic potential, was investigated in a wound-healing migration assay (Fig. 3C,D). LM8-*lacZ* cells were cultured in the absence (control cells) or in the presence of indicated concentrations of honokiol for 3 hours before wounds were applied and measured.

Wounded control cells and honokiol-treated cells were then incubated for an additional 20 hours under the respective prewounding conditions. Honokiol treatment dose-dependently reduced the migration rate of LM8-*lacZ* cells with an IC₅₀ value between 5 μ g/mL and 10 μ g/mL (Fig. 3C). Concentrations of honokiol ≥ 15 μ g/mL inhibited migration almost completely. This was in agreement with the observed suppression of metabolic activity in LM8-*lacZ* cells at these honokiol concentrations. It is noteworthy that cells treated with 15 μ g/mL honokiol remained attached at the border of the wound but rounded up and had partial loss of cell-cell contacts (Fig. 3D).

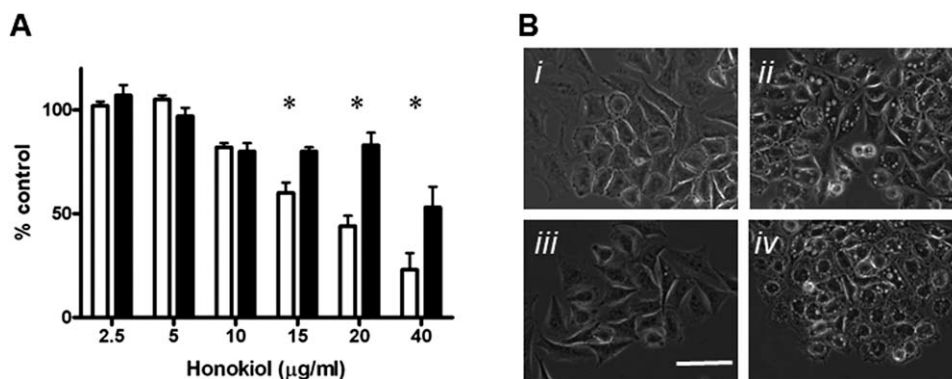


Figure 4. Honokiol inhibits metabolic activity and causes cytoplasmic vacuolation in β -galactosidase bacterial gene (*lacZ*)-expressing LM8 mouse osteosarcoma (LM8-*lacZ*) cells in vitro. (A) Dose-dependent inhibition of metabolic activity by honokiol in cells that were preincubated in the absence (open bars) or in the presence (solid bars) of 10 μ M cyclosporin A was assessed with the WST-1 reagent as described in the text (see Materials and Methods). The results expressed as the percentage of nonhonokiol-treated controls are the means \pm standard error of the mean from 6 independent experiments. Asterisks indicate $P < .05$ compared with the effects of honokiol alone. (B) These are representative phase-contrast microscopic images of cells that were (i, iii) left untreated or (ii, iv) treated with 15 μ g/mL honokiol for 2 hours after preincubation for 2 hours (i, ii) in the absence or (iii, iv) in the presence of 10 μ M cyclosporin A. Scale bar = 50 μ m in B.

Honokiol Provokes Fast Cell Death, Partially Inhibited by Cyclosporin A, and Concomitant Cytoplasmic Vacuolation With No Signs of Apoptosis or Necrosis

The results from the proliferation and migration experiments suggested that honokiol inhibited key cellular activities faster than initially demonstrated in the current study and in previous studies with cell lines of various tumor types. Consequently, we reinvestigated the metabolic response of LM8-*lacZ* cells to honokiol with the WST-1 assay and shortened the treatment from 72 hours to 4 hours. It is worth noting that these short-time incubations with honokiol inhibited the metabolic activity of LM8-*lacZ* cells almost as effectively as the 72-hour treatment. This was reflected by an IC_{50} value for honokiol of 15 μ g/mL, which was only 2 times higher than that observed for the 72-hour treatment (Fig. 4A, Table 1) and, again, was representative of the other cell types that initially were investigated with the 72-hour protocol.

It has been demonstrated that cyclosporin A protects against honokiol-induced cell death in esophageal carcinoma, breast cancer, and acute myeloid leukemia cells.^{25,26} Likewise, we also observed this effect with LM8-*lacZ* cells. The inhibition of metabolic activity by honokiol could be reversed in part by preincubation of the cells with 10 μ M cyclosporin A for 2 hours (Fig. 4A). Microscopic inspection of the cells as early as 1 hour after the beginning of honokiol treatment revealed extensive cytoplasmic vacuolation (Fig. 4Bii), which also has been

reported in human leukemia cells.^{26,27} It is noteworthy that the vacuolation provoked by 15 μ g/mL honokiol could not be prevented by a 2-hour pretreatment of LM8-*lacZ* cells with 10 μ M cyclosporin A (Fig. 4Biv). Cyclosporin A alone had no effect on cell morphology (Fig. 4Biii). All observations taken together suggested that rapid inhibition of metabolic activity and early vacuolation in honokiol-treated LM8-*lacZ* cells were not interdependent.

To further exclude the possibility that the unexpected observation of honokiol-evoked vacuolation was related to apoptosis or necrosis, we induced apoptosis in LM8-*LacZ* cells with staurosporine and induced necrosis with H_2O_2 to compare morphologic and nuclear changes in these cells with the changes in cells that were treated with honokiol. Incubation of LM8-*LacZ* cells with 1 μ M staurosporine for 6 hours induced apoptosis, as indicated by cell rounding, the formation of apoptotic bodies, chromatin condensation observed by 4',6-diamidino-2-phenylindole (DAPI) staining, and karyopyknosis revealed by a 24% reduction of the nuclear area compared with control cells ($P < .0001$; results not shown). The treatment of LM8-*LacZ* cells with 1 mM H_2O_2 for 6 hours also resulted in cell rounding and in uptake of propidium iodide in >95% of the cells, indicating loss of membrane integrity and necrosis (results not shown). Apoptotic bodies were not observed. The percentage of propidium iodide-stained control cells and staurosporine-treated cells was <1% and <5%, respectively, of the percentage of

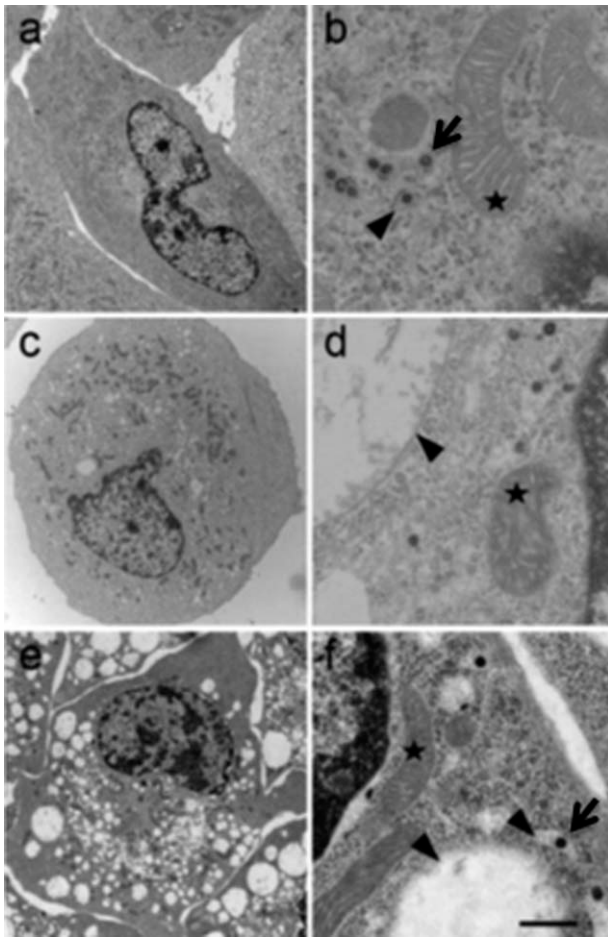


Figure 5. Honokiol-provoked vacuolation in β -galactosidase bacterial gene (*lacZ*)-expressing LM8 mouse osteosarcoma (LM8-*lacZ*) cells was observed by transmission electron microscopy. Cells were (a,b) left untreated or (c,d) treated with 15 $\mu\text{g}/\text{mL}$ honokiol for 1.5 hours; (e,f) 6 hours. Arrowheads indicate endoplasmic reticulum; arrows, viral particles; asterisks, mitochondria. Scale bar = 5 μm in a, c, and e; 0.5 μm in b, d, and f.

cells recognized in H_2O_2 -treated cells. It is important to note that the vacuoles observed in honokiol-treated cells were not observed in cells that were incubated with staurosporine or H_2O_2 . All of these findings taken together indicate that honokiol-provoked vacuolation and cell death in LM8-*LacZ* cells is unrelated to necrosis and apoptosis.

Honokiol Induces Morphologic Changes in the Endoplasmic Reticulum and in Mitochondria

The subcellular morphologic changes observed after treatment of LM8-*lacZ* cells with honokiol were investigated further by transmission electron microscopy (Fig. 5). LM8-*lacZ* cells that were treated with 15 $\mu\text{g}/\text{mL}$ honokiol for 1.5 hours had vacuoles in the cytoplasm that varied

considerably in size and measured up to 5 μm in greatest dimension (Fig. 5c,d). The ultrastructure of these vacuoles, which increased in size and number during honokiol treatment for up to 6 hours, showed enlarged, swollen endoplasmic lumen (Fig. 5d,f). Cells that were treated with 15 $\mu\text{g}/\text{mL}$ honokiol for 1.5 hours and 6 hours also had changes in the morphology of cristae in mitochondria (Fig. 5b,d,f) that appeared well organized in nontreated cells (Fig. 5b). The morphology of the nuclei and the cytoplasm, conversely, was indistinguishable in nontreated and honokiol-treated LM8-*lacZ* cells. Moreover, honokiol-treated cells did not have damaged cell membranes or cytoplasm, indicators of necrosis, or condensed nuclear DNA and an electron-dense cytoplasm characteristic of apoptosis, or autophagosomes with visible cellular or membranous constituents that would point to autophagy. Thus, honokiol dose-dependently provoked rapid cell damage and eventually cell death of highly malignant osteosarcoma cells in vitro by triggering cell destructive processes different from the well characterized cascades of mechanisms that can cause cell death.

Unexpectedly, in both treated and nontreated LM8-*lacZ* cells, retroviral particles were observed in the endoplasmic reticulum (Fig. 5b,f, arrows), but budding viruses at the plasma membrane or in the extracellular space were not observed. These findings were consistent with those from previous morphologic studies in Dunn cells,²⁸ which are the parental cells of the LM8 cell line.

DISCUSSION

In the current study, the therapeutic effect of honokiol on osteosarcoma primary tumor growth and spontaneous lung and liver metastasis was examined in a syngeneic LM8/C3H mouse model,²² which was refined in our laboratory.²³ The cytotoxic activity of honokiol was investigated further in vitro in 8 human and 2 murine osteosarcoma cell lines with various metastatic potential, reflecting in part the heterogeneity of cell populations present in primary osteosarcoma tumor tissue. The results indicated indistinguishable cytotoxic potential of honokiol in all osteosarcoma cell lines that we investigated. Therefore, the highly metastatic LM8 mouse osteosarcoma cell line that we used in the in vivo study was considered representative of all cell lines in additional experiments investigating in vitro antineoplastic properties of honokiol and mechanistic aspects.

The treatment of mice suffering from subcutaneous LM8-*LacZ* cell-derived primary tumors and spontaneous

metastases in the lung and liver with honokiol revealed unexpected findings. However, these findings were comparable to those obtained in the LM8/C3H model with parthenolide, a natural inhibitor of nuclear factor- κ B.²⁹ In that model, primary tumor growth also was not affected by intraperitoneal administration of the compound, whereas lung metastasis was reduced when parthenolide was administered concurrently with tumor cell injection. By contrast, the ability of honokiol to inhibit primary tumor growth has been demonstrated in subcutaneous xenograft models of colorectal carcinoma,¹⁴ breast cancer,¹⁷ and gastric cancer.¹⁸ It is noteworthy that the concentration of honokiol used in these 3 studies was either slightly lower or comparable to the dose administered in the current study. In a recent preliminary pharmacologic study in our laboratory in BALB/c mice, intraperitoneal administration of 150 mg/kg honokiol revealed plasma levels between 38 μ g/mL and 90 μ g/mL at 1 hour and between 9 μ g/mL and 22 μ g/mL 3 hours after injection of the compound (unpublished results). This is consistent with an estimated half-life of 1 hour assuming first-order kinetics for the clearance of honokiol from the circulation. Although the possibility cannot be excluded that honokiol has a longer half-life in BALB/c mice than in C3H mice, the data obtained in BALB/c mice provide good evidence that, in the current study, the concentrations of honokiol in the circulation during the first 2 hours after administration were within the cytotoxic range of the compound assessed in vitro for 4-hour and 45-hour treatments. Consequently, metastasizing LM8-*lacZ* cells in the circulation and in well vascularized liver and lung tissue were exposed to honokiol concentrations that affected their viability; however, the concentrations in the already established subcutaneous LM8-*lacZ* cell-derived primary tumor may have been too low and the time of exposure too short to cause cell death. To this end, the results of a recent study indicated that honokiol administered intravenously reached the highest levels in the lung, followed by the levels measured in the circulation and in the liver.³⁰ These data support the hypothesis that honokiol treatment applied in the current study mainly affected metastasizing cells in the circulation and, notably, in the lung early during primary tumor development. This likely explains the predominant suppressive effect of honokiol on the formation of macrometastases, which presumably arose from early metastasizing cells. Accordingly, at the dose used in the current study, honokiol appears to become less effective during unlimited late progression of the primary tumor, resulting in an overflow of metastasiz-

ing cells in the circulation and, consequently, in numerous micrometastases in the lung and the liver, which may be inhibited in outgrowth because of some saturation of the tissue with honokiol.

Encouraged by the promising antimetastatic activity of honokiol in the LM8/C3H mouse osteosarcoma model, we investigated the cytotoxicity of honokiol in a variety of osteosarcoma cell lines that differed in their metastatic activity and, to some extent, represented the heterogeneity of tumor cells in osteosarcoma. The sensitivity of the investigated osteosarcoma cell lines to honokiol was within the range of that reported previously for other human tumor cell lines, such as lung cancer cells¹³ and colorectal carcinoma cells.¹⁴ Remarkably, we observed that the osteosarcoma cell lines with high in vivo metastatic potential were equally sensitive or even more sensitive to the cytotoxic effects of honokiol than their respective low-metastatic parental cell lines. These findings differ from those from a previous study, in which the resistance of MG63 and MG63 M8 cells to cisplatin, doxorubicin, and etoposide reportedly was correlated with increasing metastatic potential.³¹

Reduced activity of mitochondrial dehydrogenases compared with controls, as assessed with the WST-1 assay in cells that were treated with honokiol for several hours, can indicate inhibition of cell proliferation or a cytotoxic response that causes cell death. Our findings in LM8-*lacZ* cells demonstrate that honokiol at concentrations <10 μ g/mL inhibited proliferation in a dose-dependent and reversible manner, as demonstrated in the experiments that examined the recovery of LM8-*lacZ* cells from honokiol treatment. Concentrations >10 μ g/mL caused cell death, as indicated by the lower cell density at the end of the experiment compared with the density after cell seeding. The threshold of 10 μ g/mL between antiproliferative and cytotoxic activity of honokiol in LM8-*lacZ* cells was confirmed in the wound-healing migration experiments.

Studies investigating the mechanism(s) of action of honokiol have demonstrated apoptotic activity in cells of different tumor types,^{9,11,13,16} but necrosis and induction of autophagy also have been reported (for review, see Fried et al³²). Here, cytotoxic concentrations of honokiol caused rapid subcellular morphologic changes in LM8-*lacZ* cells that were recognized by phase-contrast and transmission electron microscopy. Most prominent but atypical changes for apoptosis, autophagy, and necrosis were recognized as early as 1.5 hours after the beginning of honokiol treatment and included swelling of the endoplasmic reticulum and disintegration into cytoplasmic

vacuoles and morphologically altered mitochondria with distorted and enlarged cisternae. Rapid vacuolation provoked by honokiol also was observed in almost all of the osteosarcoma cell lines listed in Table 1 of this study (results not shown). Vacuolation and mitochondrial morphologic changes, together with some necrotic features, also have been observed in human HL60 leukemia cells upon treatment with 15 $\mu\text{g}/\text{mL}$ honokiol for 6 hours.²⁶ It is noteworthy that, in HL60 cells, cell death was inhibited almost completely by cyclosporin A, an inhibitor of cyclophilin D, which is a component of the mitochondrial permeability transition pore. A key role of the mitochondrial permeability transition pore in honokiol-induced cytotoxicity also was described for esophageal adenocarcinoma cells.²⁵ In the currently investigated LM8-*lacZ* cells, cyclosporin A indeed also reversed in part the honokiol dose-dependent decrease in mitochondrial activity, but vacuolation was not affected by cyclosporin A. It is important to note that these experiments also revealed that the metabolic activity-inhibitory potency of honokiol decreased only 2-fold when the treatment period was reduced from 72 hours to 4 hours. All of these observations together suggest that honokiol, when applied in vitro at cytotoxic concentrations to LM8-*lacZ* cells, evokes very rapid, irreversible damage in the endoplasmic reticulum and in mitochondria that leads to rapid cell death distinct from apoptosis and/or autophagy.

In conclusion, honokiol is a rather potent antimetastatic compound in the syngeneic LM8/C3H mouse osteosarcoma model. In vitro, honokiol evokes cytotoxic effects in osteosarcoma cells distinct from apoptosis, necrosis, and autophagy. Further studies in vitro and in vivo are needed to investigate how honokiol affects primary tumor growth and metastasis of osteosarcoma in combination with conventional drugs in an orthotopic osteosarcoma mouse model. Considering the reported lack of severe side effects of honokiol in animals and in humans and the predominant antimetastatic activity demonstrated in the current study, honokiol appears to be a promising novel chemotherapeutic agent for the treatment of osteosarcoma particularly in patients who have metastases at diagnosis and a poor prognosis.

FUNDING SOURCES

This study was supported by the Swiss National Science Foundation (SNF); the Schweizerischer Verein Balgrist; the University of Zurich; the Krebsliga Zurich; a grant from the Walter L. and

Johanna Wolf Foundation, Zurich, Switzerland; the Margolis Foundation; and the Atlanta Veterans Administration Medical Center.

CONFLICT OF INTEREST DISCLOSURES

The authors made no disclosures.

REFERENCES

1. Longhi A, Errani C, De Paolis M, Mercuri M, Bacci G. Primary bone osteosarcoma in the pediatric age: state of the art. *Cancer Treat Rev*. 2006;32:423-436.
2. Marina N, Gebhardt M, Teot L, Gorlick R. Biology and therapeutic advances for pediatric osteosarcoma. *Oncologist*. 2004;9:422-441.
3. Tsai SK, Huang CH, Huang SS, Hung LM, Hong CY. Antiarrhythmic effect of magnolol and honokiol during acute phase of coronary occlusion in anesthetized rats: influence of L-NAME and aspirin. *Pharmacology*. 1999;59:227-233.
4. Tsai SK, Huang SS, Hong CY. Myocardial protective effect of honokiol: an active component in *Magnolia officinalis*. *Planta Med*. 1996;62:503-506.
5. Ho KY, Tsai CC, Chen CP, Huang JS, Lin CC. Antimicrobial activity of honokiol and magnolol isolated from *Magnolia officinalis*. *Phytother Res*. 2001;15:139-141.
6. Chiang CK, Sheu ML, Hung KY, Wu KD, Liu SH. Honokiol, a small molecular weight natural product, alleviates experimental mesangial proliferative glomerulonephritis. *Kidney Int*. 2006;70:682-689.
7. Ou HC, Chou FP, Lin TM, Yang CH, Sheu WH. Protective effects of honokiol against oxidized LDL-induced cytotoxicity and adhesion molecule expression in endothelial cells. *Chem Biol Interact*. 2006;161:1-13.
8. Bai X, Cerimele F, Ushio-Fukai M, et al. Honokiol, a small molecular weight natural product, inhibits angiogenesis in vitro and tumor growth in vivo. *J Biol Chem*. 2003;278:35501-35507.
9. Ishitsuka K, Hideshima T, Hamasaki M, et al. Honokiol overcomes conventional drug resistance in human multiple myeloma by induction of caspase-dependent and -independent apoptosis. *Blood*. 2005;106:1794-1800.
10. Nagase H, Ikeda K, Sakai Y. Inhibitory effect of magnolol and honokiol from *Magnolia obovata* on human fibrosarcoma HT-1080. Invasiveness in vitro. *Planta Med*. 2001;67:705-708.
11. Battle TE, Arbiser J, Frank DA. The natural product honokiol induces caspase-dependent apoptosis in B-cell chronic lymphocytic leukemia (B-CLL) cells. *Blood*. 2005;106:690-697.
12. Hibasami H, Achiwa Y, Katsuzaki H, et al. Honokiol induces apoptosis in human lymphoid leukemia Molt 4B cells. *Int J Mol Med*. 1998;2:671-673.
13. Yang SE, Hsieh MT, Tsai TH, Hsu SL. Down-modulation of Bcl-XL, release of cytochrome c and sequential activation of caspases during honokiol-induced apoptosis in human squamous lung cancer CH27 cells. *Biochem Pharmacol*. 2002;63:1641-1651.
14. Chen F, Wang T, Wu YF, et al. Honokiol: a potent chemotherapy candidate for human colorectal carcinoma. *World J Gastroenterol*. 2004;10:3459-3463.

15. Wang T, Chen F, Chen Z, et al. Honokiol induces apoptosis through p53-independent pathway in human colorectal cell line RKO. *World J Gastroenterol.* 2004;10:2205-2208.
16. Shigemura K, Arbiser JL, Sun SY, et al. Honokiol, a natural plant product, inhibits the bone metastatic growth of human prostate cancer cells. *Cancer.* 2007;109:1279-1289.
17. Wolf I, O'Kelly J, Wakimoto N, et al. Honokiol, a natural biphenyl, inhibits in vitro and in vivo growth of breast cancer through induction of apoptosis and cell cycle arrest. *Int J Oncol.* 2007;30:1529-1537.
18. Sheu ML, Liu SH, Lan KH. Honokiol induces calpain-mediated glucose-regulated protein-94 cleavage and apoptosis in human gastric cancer cells and reduces tumor growth [serial online]. *PLoS ONE.* 2007;2:e1096.
19. Kuribara H, Kishi E, Hattori N, Okada M, Maruyama Y. The anxiolytic effect of 2 oriental herbal drugs in Japan attributed to honokiol from magnolia bark. *J Pharm Pharmacol.* 2000;52:1425-1429.
20. Kuribara H, Stavinoha WB, Maruyama Y. Behavioural pharmacological characteristics of honokiol, an anxiolytic agent present in extracts of Magnolia bark, evaluated by an elevated plus-maze test in mice. *J Pharm Pharmacol.* 1998;50:819-826.
21. Mitta B, Rimann M, Fussenegger M. Detailed design and comparative analysis of protocols for optimized production of high-performance HIV-1-derived lentiviral particles. *Metab Eng.* 2005;7:426-436.
22. Asai T, Ueda T, Itoh K, et al. Establishment and characterization of a murine osteosarcoma cell line (LM8) with high metastatic potential to the lung. *Int J Cancer.* 1998;76:418-422.
23. Arlt MJ, Banke IJ, Walters DK, et al. LacZ transgene expression in the subcutaneous Dunn/LM8 osteosarcoma mouse model allows for the identification of micrometastasis. *J Orthop Res.* 2011;29:938-946.
24. Fidler IJ, Kripke ML. Metastasis results from preexisting variant cells within a malignant tumor. *Science.* 1977;197:893-895.
25. Chen G, Izzo J, Demizu Y, et al. Different redox states in malignant and nonmalignant esophageal epithelial cells and differential cytotoxic responses to bile acid and honokiol. *Antioxid Redox Signal.* 2009;11:1083-1095.
26. Li L, Han W, Gu Y, et al. Honokiol induces a necrotic cell death through the mitochondrial permeability transition pore. *Cancer Res.* 2007;67:4894-4903.
27. Wang Y, Yang Z, Zhao X. Honokiol induces paraptosis and apoptosis and exhibits schedule-dependent synergy in combination with imatinib in human leukemia cells. *Toxicol Mech Methods.* 2010;20:234-241.
28. Urist MR, Nakata N, Felsler JM, et al. An osteosarcoma cell and matrix retained morphogen for normal bone formation. *Clin Orthop Relat Res.* 1977;124:251-266.
29. Kishida Y, Yoshikawa H, Myoui A. Parthenolide, a natural inhibitor of nuclear factor-kappaB, inhibits lung colonization of murine osteosarcoma cells. *Clin Cancer Res.* 2007;13:59-67.
30. Wang X, Duan X, Yang G, et al. Honokiol Crosses BBB and BCSFB, and Inhibits Brain Tumor Growth in Rat 9L Intracerebral Gliosarcoma Model and Human U251 Xenograft Glioma Model. *PLoS One.* 2011;6:e18490.
31. Walters DK, Steinmann P, Langsam B, Schmutz S, Born W, Fuchs B. Identification of potential chemoresistance genes in osteosarcoma. *Anticancer Res.* 2008;28:673-679.
32. Fried LE, Arbiser JL. Honokiol, a multifunctional antiangiogenic and antitumor agent. *Antioxid Redox Signal.* 2009;11:1139-1148.